

Fabrication of carbon papers using polyacrylonitrile fibers as a binder

Hyunuk Kim · Young-Ju Lee · Sung-Jin Lee ·
Yong-Sik Chung · Yoonjong Yoo

Received: 21 November 2013 / Accepted: 29 January 2014 / Published online: 13 February 2014
© Springer Science+Business Media New York 2014

Abstract Carbon papers (CPs) have been fabricated using wet-laying carbon fibers (CFs) and polyacrylonitrile (PAN) fibers. Scanning electron microscopy revealed that the PAN fibers tightly interconnected the CF junctions with the pores between the fibers. The tensile strength of the carbon webs (CWs) increased as the fraction of PAN fibers used as the binder increased. The CW fabricated with 0.15 wt% PAN fibers had a tensile strength six times greater than that of the CW without PAN fibers. Moreover, by mixing the CFs with PAN fibers in water, the CFs separated from each other in the webs due to the interruption of hydrophobicity between the CFs. After mixing with PAN fibers, the CWs were carbonized at 1200 °C in the presence of a phenolic resin. The PAN fibers maintained their morphology due to their high carbon content after carbonization. The electrical resistivity of the CPs with high PAN fiber content was significantly lower than that of a CP without PAN fibers due to the interconnection of the CFs by the carbonized PAN fibers.

Introduction

Carbon papers (CPs) have been widely investigated as gas diffusion layers in proton exchange membrane fuel cells due to their high electrical conductivity and gas permeability [1–6]. In general, CPs are prepared from the high-temperature pyrolysis of preformed carbon webs (CWs) covered with a phenolic resin. Prior to pyrolysis with a phenolic resin, the preformed CWs assembled by wet-laying carbon fibers (CFs) are too weak for fabrication in a continuous production process. The tensile strength of the CWs is a particular problem. To overcome this obstacle, chemical binders have been added to the CF solutions. Jabbour and co-workers used microfibrillated cellulose (MFC) as a binder in an aqueous suspension to produce flexible paper-like electrodes for Li-ion batteries [7]. Scanning electron microscopy (SEM) revealed that hydrogen bonding within the MFC induced the formation of a porous web-like structure in the graphite/MFC film. More recently, the authors used bleached eucalyptus kraft cellulose fibers (BEKCF) as a novel binder for CF composite papers [8]. The CFs were held together by a homogeneous BEKCF network. Increasing the BEKCF weight fraction in the composite sheet, improved the mechanical properties of the paper. Yan and co-workers reported the fabrication of carbon nanofiber–polyaniline composite flexible paper using a facile polymerization of aniline monomers on the CNT paper [9]. The composite paper showed improved electrical conductivity and electrochemical performances compared with the CNT paper.

Polyacrylonitrile (PAN) fibers are a well-known precursor for the synthesis of CFs due to their high carbon yield and melting point [10]. High-temperature thermal treatment converts the precursor PAN fibers into graphitic CFs. This PAN-based CF is significantly stronger than the CFs derived from pitch, rayon, and other materials [11]. The high strength

Electronic supplementary material The online version of this article (doi:10.1007/s10853-014-8096-4) contains supplementary material, which is available to authorized users.

H. Kim (✉) · Y.-J. Lee · S.-J. Lee · Y. Yoo
Energy Materials Laboratory, Korea Institute of Energy
Research, Daejeon 305-343, Republic of Korea
e-mail: hyunuk@kier.re.kr

Y. Yoo
e-mail: yjyou@kier.re.kr

Y.-S. Chung
Department of Textile Engineering, Chonbuk National
University, Jeonju 561-756, Republic of Korea
e-mail: psdcolor@jbnu.ac.kr

of the CFs derived from the PAN fibers motivated our study of the incorporation of PAN fibers into the CWs as a binder to increase their tensile strength. Herein, we report the fabrication of CPs using a wet-laying process with PAN-based CFs and PAN fibers as the binder. The PAN fibers played roles not only to prevent the aggregation of the PAN-based CFs but also to increase the tensile strength of the CWs. The tensile strength of the CWs with a significant fraction of PAN fibers was significantly higher than that of the CW without PAN fibers. In addition, after the pyrolysis of the CWs at 1200 °C in the presence of a phenolic resin, the electrical resistivity of the CPs with a significant fraction of PAN fibers was significantly lower than that of the CP without PAN fibers due to the interconnection of the CFs by the carbonized PAN fibers.

Experimental

Materials and instruments

The PAN-based CFs, branded as T700, were manufactured by the Toray Co., Ltd. (Nasushiobara-shi, Tochigi, Japan). These CFs were chopped with a length of 4.5 mm and purchased from ACE C & TECH Co., Ltd. (Seoul, South Korea). The nominal diameter of CFs is approximately 8.5 μm. The polyvinyl alcohol (PVA) flakes with DP 2000 were purchased from Kuraray Chemical Co., Ltd. (Osaka, Japan). Dimethyl sulfoxide (DMSO) and methanol were purchased from Samchun Pure Chemical Co., Ltd. (Pyungtak-si, Gyeonggi-do, South Korea). Sodium carboxymethyl cellulose (Na-CMC) with the molecular weight of 300000 and the phenolic resin (KRD-HM2) were purchased from KOREA CMC Co., Ltd. (Daejeon-si, South Korea) and KOLON Industries, Inc. (Gwacheon-si, Gyeonggi-do, South Korea), respectively.

The SEM images were acquired on a HITACHI S-4800 at an acceleration voltage of 5 kV. The thermogravimetric analysis (TGA) data were obtained using a TA 2050 instrument with a heating rate of 10 °C/min up to 1000 °C. The X-ray photoelectron spectra (XPS) were obtained on an AXIS-NOVA (KRATOS Analytical, UK) with a monochromatic Al K α X-ray source operating at 15 kV and 10 mA. The XPS spectra were deconvoluted using the “Fitt” software as an XPS curve-fitting program to determine the chemical state and number of functional groups.

Preparation of the PAN fibers

The PAN fibers were prepared by phase separating the PAN from the PVA [12]. The PAN (18 wt%) and PVA (15 wt%) were dissolved at 50 °C for 24 h and 110 °C for 4 h, respectively, in DMSO. Next, the PAN and PVA

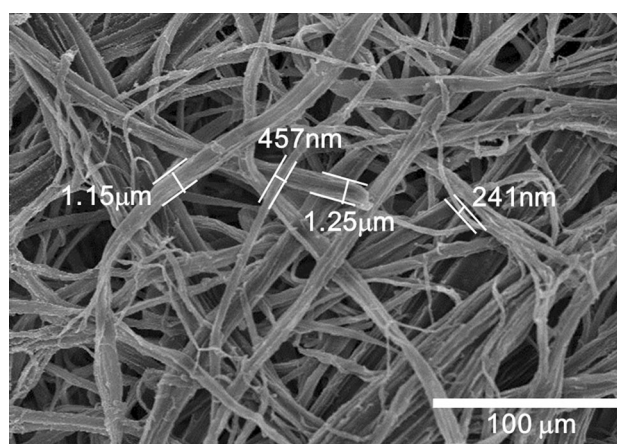


Fig. 1 SEM image of the PAN fibers

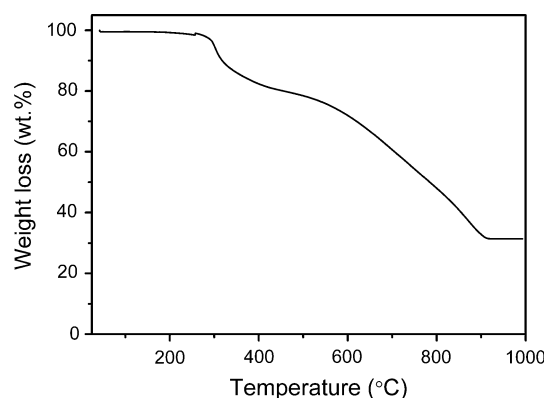


Fig. 2 TGA data of the PAN fibers

solutions were combined in a weight ratio of 5:5. A wet-spinning instrument was specially designed in our lab for the PAN:PVA composite fibers. The PAN/PVA mixture in DMSO was directly spun into a methanol coagulation bath at 25 °C through a spinneret with 150 holes measuring 0.1 mm in diameter. To establish the fiber orientation, the fibers were elongated sixfold using a drawing roller and washed with water at 100 °C to remove the PVA. As observed in the SEM image in Fig. 1, the PAN fibers were several micrometers in thickness. The TGA data revealed that the PAN fibers decomposed at temperatures above 260 °C, losing 68 wt% of their total weight up to 900 °C. Above 900 °C, no significant weight loss occurred (Fig. 2).

Preparation of the CWs

The NaCMC (12 g, 0.6 wt%) was added to H₂O (2 L) to increase the viscosity, and the solution was stirred for 1 day at room temperature at 1000 rpm. The dynamic viscosity of the solution was measured to be 145.2 cP at

28.5 °C using a Brookfield viscometer with an LV-1 spindle. After completely dissolving the NaCMC in H₂O, the chopped PAN-CFs (2 g, corresponding to 0.1 wt% in H₂O) and various quantities of PAN fibers (corresponding to 0.05, 0.1, and 0.15 wt% in H₂O) were added and stirred

for 2 h at 1500 rpm. Each solution was then filtered using a fine screen with a 0.11 × 0.18-mm² mesh (Ultra 5000-XK574, Albany International Corp.) and dried at 90 °C. According to the SEM images of the CWs in Fig. 3, the CFs without PAN fibers were unidirectionally aligned.

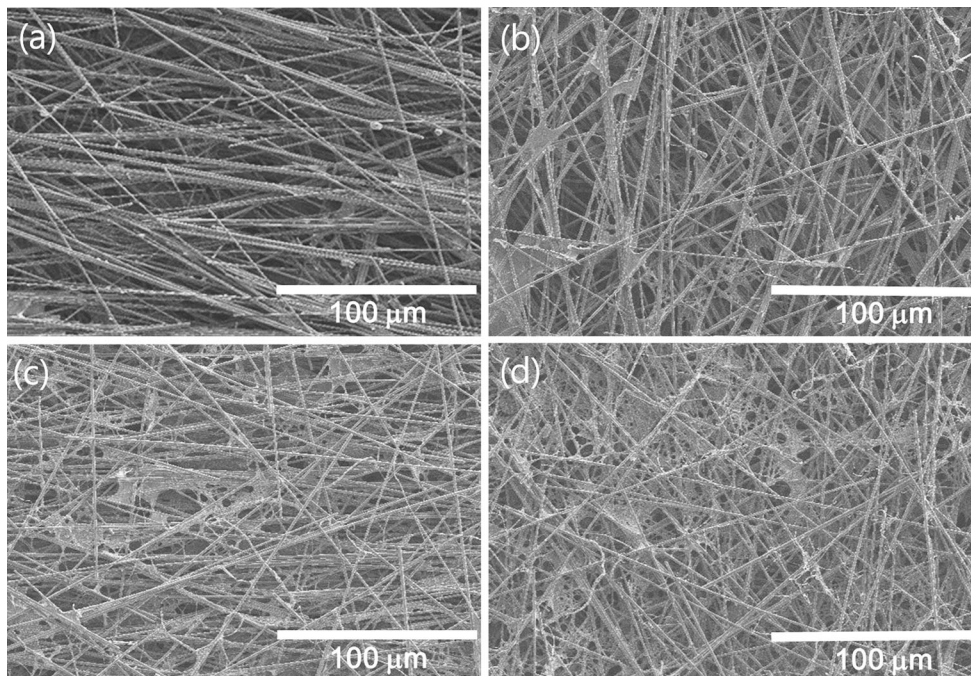


Fig. 3 SEM images of the CWs **a** without PAN fibers and with **b** 0.05, **c** 0.1, and **d** 0.15 wt% PAN fibers

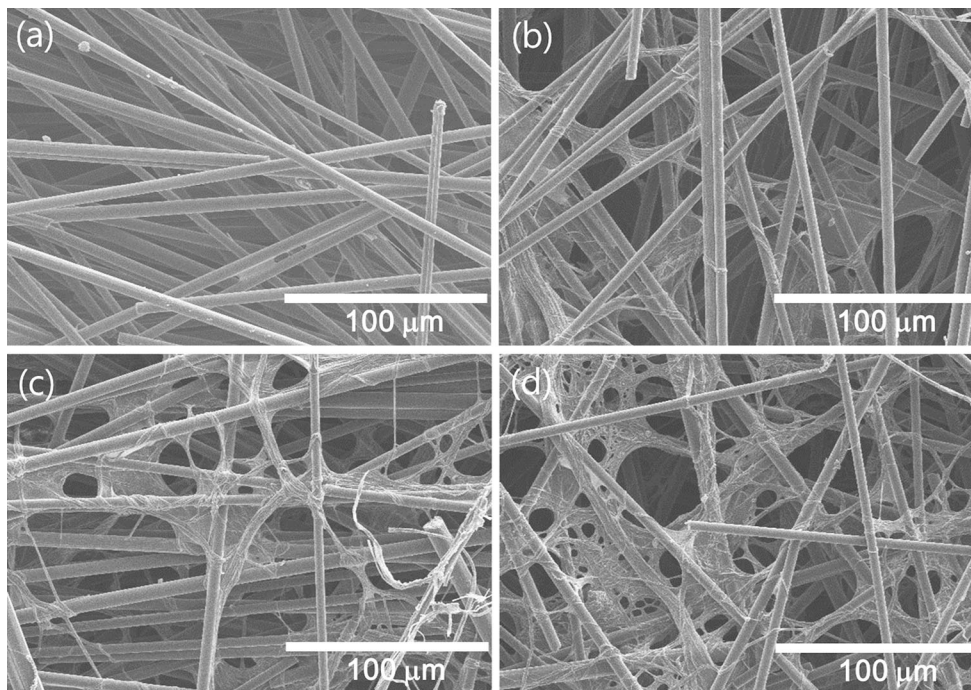


Fig. 4 SEM images of the CWs **a** with no addition of PAN fibers and with addition of **b** 0.05 wt%, **c** 0.1 wt%, and **d** 0.15 wt% PAN fibers

In contrast, those with PAN fibers were randomly distributed because the PAN fibers prevented CF aggregation. The porosity of the CWs was measured by mercury intrusion porosimetry (AutoPore IV 9500, Micromeritics). In addition, the gas permeability of CWs was measured using an air permeability tester (A20, Borgwaldt KC), which is in compliance to ISO 2965.

Tensile strength of the CWs

The tensile properties of the CWs were measured on a Tinius Olsen H5KT benchtop tensile tester with a 50-N load cell and a crosshead speed of 1 mm/min at room temperature under ambient humidity. Sheets of CWs ($2.5 \times 24 \text{ cm}^2$) were affixed to the two machine grips with a support span of 180 mm and pulled until the samples broke. Stress–strain curves of CWs with PAN fibers were plotted (Fig. S1). The maximum of the stress–strain curve was defined as the tensile strength (Eq. 1). Each

measurement was repeated three times to obtain an average value.

$$TS = \frac{F}{A} \quad (1)$$

The term *TS* is the tensile strength (MPa), *F* is the maximum load (N), and *A* is the cross-sectional area (mm^2).

Preparation of the CPs

To improve the electrical conductivity of the CWs with electrical resistivity of a few hundred $\text{m}\Omega \text{ cm}^2$, the CWs combined with the PAN fibers were coated with a phenolic resin [13]. The CWs with PAN fibers were immersed in a phenolic resin solution diluted with methanol (resin:methanol = 1:6 w/w) for 5 min, then dried at room temperature. The webs were heated at a rate of $5 \text{ }^\circ\text{C}/\text{min}$ and carbonized at $1200 \text{ }^\circ\text{C}$ for 90 min under a N_2 atmosphere.

Table 1 The properties of the CWs entangled with PAN fibers

Percentage of PAN fibers	Basis weight (g/m^2)	Thickness (mm)	Tensile strength (MPa)	Gas permeability $\text{mL}/(\text{cm}^2 \text{ s})$	Porosity (%)
0	29.05	0.190	0.436 ± 0.233	823.9	94.4210
0.05	32.22	0.221	1.661 ± 0.198	547.8	90.4676
0.10	32.86	0.186	2.343 ± 0.794	398.6	89.8642
0.15	35.40	0.206	2.511 ± 0.125	268.9	87.8183

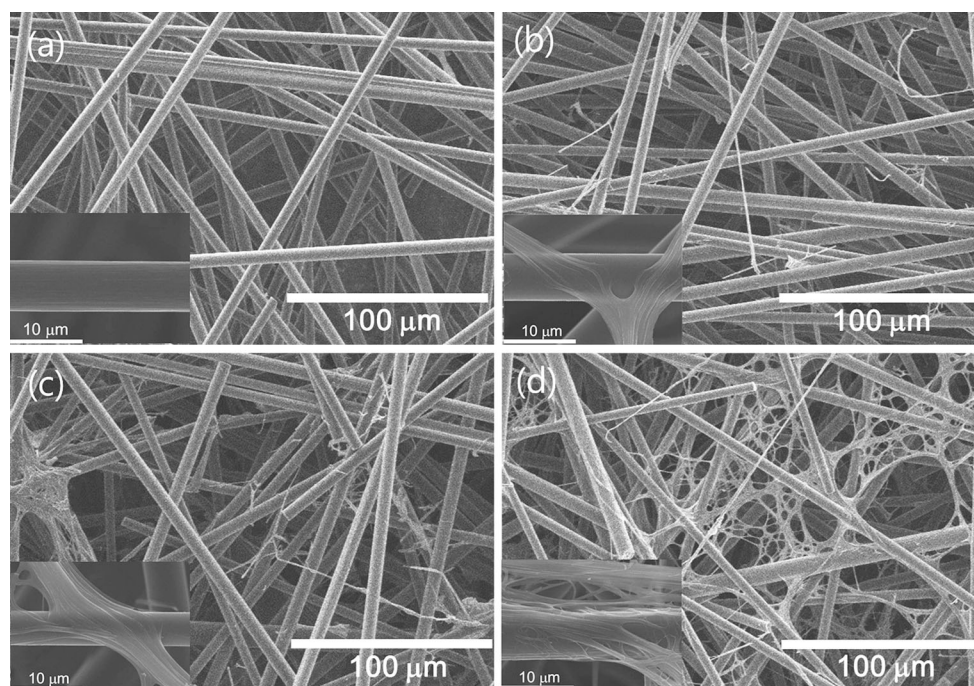


Fig. 5 SEM images of the CWs after pyrolysis ($\times 500$) **a** without PAN fibers and with **b** 0.05, **c** 0.1, and **d** 0.15 wt% PAN fibers. *Inset* magnified images of the CFs

The CWs with PAN fibers were carbonized under the same conditions used for pyrolysis with a phenolic resin solution to confirm that the PAN fiber morphology was maintained.

Electrical resistivity of the CPs

The donut-shaped CPs with an area of 4.799 cm² were prepared and placed between two gold electrodes. The thickness and electrical resistance of CPs were simultaneously measured using a gas diffusion layer (GDL) property analyzer (CPRT 10 L, LivingCare). The electrical resistance (Ω) was multiplied by a CP area (cm²) to calculate the electrical resistivity ($\Omega \times \text{cm}^2$) (Fig. S2).

Results and discussion

Characterization of the CWs with PAN fibers

Dispersing the CFs in water is difficult because they are hydrophobic; this problem must be addressed to facilitate the preparation of CWs via the separation of CF bundles. To improve the dispersion of the CFs in water, significant effort has been devoted to design hydrophilic CFs using CF surface oxidation [14–16]. As indicated in the SEM images in Figs. 3a and 4a, the CW without PAN fibers exhibits individual CFs that were not well separated but were loosely assembled. The SEM images of the CWs with the PAN fibers demonstrate that the CFs were well separated, indicating that the PAN fibers might disrupt the CFs aggregation. In addition, PAN fibers play an important role as a binder in the CWs. When the fraction of PAN fibers in the mixture was increased, CFs were more tightly entangled by PAN fibers (Fig. 4b–d).

To investigate the mechanical properties of the CWs entangled with the PAN fibers, the tensile strengths of the samples were measured using the TAPPI test T-494, which measures the tensile breaking properties of paper using a constant rate of elongation apparatus. When 0.05 wt% PAN fiber was added to the CF solution, the tensile strength of the resulting CW was 1.661 MPa, which is 3.8 times higher than that of the conventional CW (Table 1). The tensile strength of the specimens increased with the increasing fraction of PAN fibers. At a 0.15 wt% PAN fiber content, the tensile strength of the CW reached 2.511 MPa.

To investigate whether the PAN fibers block the pores, we measured the gas permeability of the webs using an air permeability tester (A20, Borgwaldt KC). The gas permeability decreased linearly as the fraction of PAN fibers in the webs increased due to pore blockage. The porosity, determined using mercury intrusion porosimetry (WIN9400, Micromeritics), also indicated that the CWs with PAN fibers are less permeable than the CWs without PAN fibers.

However, porosities of 88–94 % are sufficiently high for fabricating CPs by mixing CWs with phenolic resin.

Characterization of the carbonized CWs

According to the PAN fiber degradation mechanism, PAN, with its open-chain structure, undergoes a cyclization reaction to form a ladder polymer at temperatures above 180 °C [17]. Further heat treatment up to 1600 °C expels the non-carbon atoms and yields a turbostratic structure

Table 2 Elemental analysis of the carbonized CWs with PAN fibers

Quantity of PAN fibers (wt%)	C (%)	H (%)	N (%)	O (%) ^a
0	96.09	0	1.97	2.56
0.05	95.80	0	1.73	3.55
0.10	96.64	0	1.55	2.62
0.15	96.25	0	1.40	2.79

^a Determined via energy-dispersive X-ray spectrometry

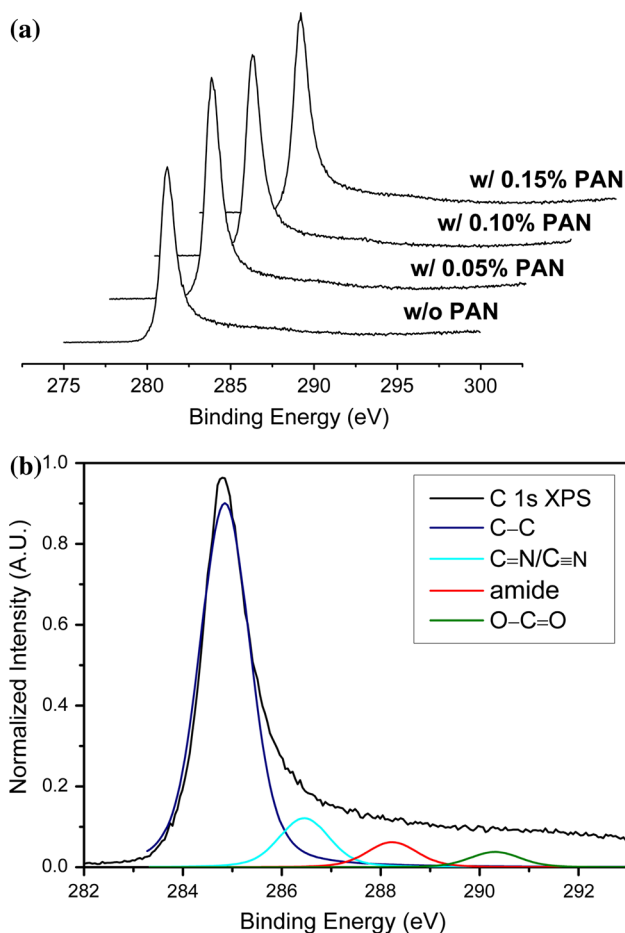


Fig. 6 **a** C 1s XPS spectra of the CWs with different fractions of PAN fibers, **b** the deconvoluted spectra of the CWs with 0.15 wt% PAN fibers

[10, 11]. As revealed in the SEM image in Fig. 5, the PAN fibers maintained their morphology after pyrolysis due to their high carbon content. Elemental analysis revealed a carbon content over 95 %, small quantities of nitrogen and oxygen, and no hydrogen (Table 2), which indicate the carbonization of PAN fibers [17].

As in the previous XPS analyses of the CFs [18–22], the C 1s XPS spectra of the CWs revealed the surface characteristics of the carbon present in the web. Figure 6 illustrates a sequence of C 1s XPS profiles recorded for the CWs with the PAN fibers. The C 1s XPS spectra of the CWs with 0.15 wt% PAN fibers were deconvoluted into four individual peaks of C=C, C=N/C≡N, amide, and O–C=O at 284.8, 286.5, 288.2, and 290.3 eV, respectively (Fig. 6b; Table 3). The graphitic carbon peak at 284.8 eV is 80.2 %, indicating the dominant formation of a

conductive pathway by overlapping *p*-orbitals [19]. The other CW compositions determined via deconvolution of the C 1s XPS spectra are listed in Table 3.

Preparation and properties of the CPs

The phenolic resin on the CW changed to a glassy carbon with high electrical conductivity and rigidity above 900 °C. As shown in Fig. 7, the CWs are fully covered by the glassy carbon, which connects the CFs. The CW is named the CP after pyrolysis of the CW with a phenolic resin at 1200 °C. PAN fibers and phenolic resin partially blocked the pores during carbonization lowering the porosity of CPs to ~80 %, but the values are higher than those of SGL 10AA, 24AA, and 34AA (Table 4) [23–25].

The electrical resistance of the CPs was measured using a gas diffusion layer (GDL) property analyzer (CPRT 10 L, LivingCare). With considering the stack clamping pressure in the PEM fuel cell, the electrical resistances were measured [26] (Fig. S2). As the fraction of PAN fibers increased, the gas permeability and porosity decreased indicating that some of the pores became blocked by the carbonized PAN fibers and phenolic resin (Table 4). Adjusting the fraction of PAN fiber may enable control over the porosity and gas permeability of the CPs. When the fraction of PAN fibers increased, the electrical resistivity of the CPs at 10 bar decreased. The flexural strength of CPs with PAN fibers is much higher than

Table 3 The compositions of the CWs with PAN fibers

Fraction of PAN fibers (wt%)	C=C at 284.8 eV	C=N/C≡N at 286.5 eV	Amide at 288.2 eV	O–C=O at 290.3 eV
0	80.2	10.8	5.4	3.6
0.05	80.0	11.2	5.4	3.4
0.10	80.5	11.0	5.2	3.3
0.15	80.2	10.8	5.6	3.4

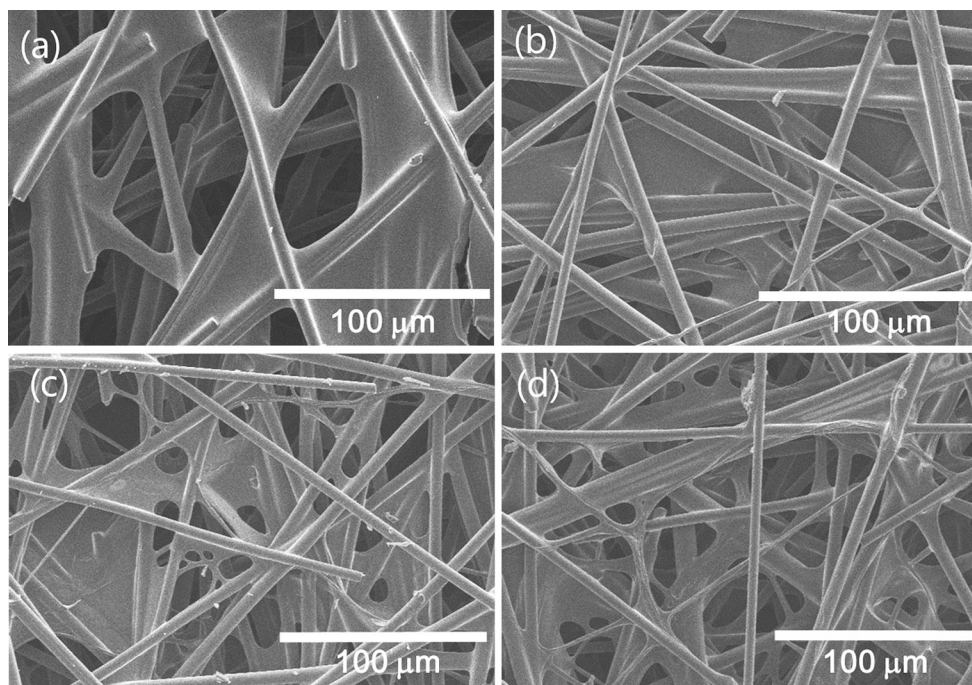


Fig. 7 SEM images of the CPs **a** without PAN fibers and with **b** 0.05 **c** 0.1, and **d** 0.15 wt% PAN fibers

Table 4 Thickness, gas permeability, and electrical resistivity of the CPs

CPs	PAN fibers (wt%)	Thickness (μm)	Gas permeability $\text{mL}/(\text{cm}^2 \text{ s})$	Porosity (%)	Electrical resistivity at 10 bar ($\text{m}\Omega \text{ cm}^2$)	Flexural strength (MPa)
This work	0	368	722.5	88.7	17.9	8.820 ± 1.041
	0.05	291	560.8	85.7	14.6	29.657 ± 11.966
	0.1	242	347.5	84.6	6.3	24.353 ± 6.069
	0.15	299	275.7	79.4	5.7	24.940 ± 4.950
10AA	–	340	159.5	73.3	2.6	8.134 ± 1.419
24AA	–	191	53.8	77.7	0.7	24.498 ± 2.274
34AA	–	301	148.3	66.4	1.9	21.198 ± 4.356

that of CP without PAN fibers. These behaviors may be attributed to the interconnection of the CFs by the carbonized PAN fibers.

Conclusions

The CPs entangled with PAN fibers were prepared via the wet laying of chopped CFs and PAN fibers. The junctions of the CFs were tightly bound by the PAN fibers, resulting in CWs with tensile strength that increased with the PAN fiber fractions. Although the CPs exhibited lower gas permeabilities at high PAN fiber contents than the CP without PAN fibers, the electrical conductivity increased due to the interconnection of the CFs by the carbonized PAN fibers. The gas permeability and conductivity values of the CPs containing significant fractions of PAN fibers are comparable to those of commercial products [27]. Therefore, we believe that fabricating CPs using PAN fibers as a novel binder in a gas diffusion medium will contribute to further improving fuel cell performance.

Acknowledgements We gratefully acknowledge the Principal Project of the Korea Institute of Energy Research (KIER) funded by the Ministry of Science, ICT & Future Planning of the Republic of Korea (B3-2413-04).

References

- Cindrella L, Kannan AM, Lin JF, Saminathan K, Ho Y, Lin CW, Wertz J (2009) Gas diffusion layer for proton exchange membrane fuel cells—a review. *J Power Sources* 194:146–160
- Martínez-Rodríguez MJ, Cui T, Shimpalee S, Seraphin S, Duong B, Van Zee JW (2012) Effect of microporous layer on MacMullin number of carbon paper gas diffusion layer. *J Power Sources* 207:91–100
- Ihonen J, Mikkola M, Lindbergh G (2004) Flooding of gas diffusion backing in PEFCs physical and electrochemical characterization. *J Electrochem Soc* 151:A1152–A1161
- Vielstich W, Lamm A, Gasteiger HA (2003) *Handbook of fuel cells: fundamentals, technology, applications*, 1st edn. Wiley, New York
- Park GG, Sohn YJ, Yang TH, Yoon YG, Lee WY, Kim CS (2004) Effect of PTFE contents in the gas diffusion media on the performance of PEMFC. *J Power Sources* 131:182–187
- Williams MV, Begg E, Bonville L, Kunz HR, Fenton JM (2004) Characterization of gas diffusion layers for PEMFC. *J Electrochem Soc* 151:A1173–A1180
- Jabbour L, Gerbaldi C, Chaussy D, Zeno E, Bodoardo S, Beneventi D (2010) Microfibrillated cellulose–graphite nanocomposites for highly flexible paper-like Li-ion battery electrodes. *J Mater Chem* 20:7344–7347
- Jabbour L, Chaussy D, Eyraud B, Beneventi D (2012) Highly conductive graphite/carbon fiber/cellulose composite papers. *Compos Sci Technol* 72:616–623
- Yan X, Tai Z, Chena J, Xue Q (2011) Fabrication of carbon nanofiber–polyaniline composite flexible paper for supercapacitor. *Nanoscale* 3:212–216
- Rahaman MSA, Ismail AF, Mustafa A (2007) A review of heat treatment on polyacrylonitrile fiber. *Polym Degrad Stab* 92:1421–1432
- Cato AD, Edie DD (2003) Flow behavior of mesophase pitch. *Carbon* 41:1411–1417
- Kim S, Chung YS, Choi HS, Jin FL, Park SJ (2013) Preparation and characterization of PAN-based superfined carbon fibers for carbon-paper applications. *Bull Korean Chem Soc* 34:3733–3737
- Mathur RB, Maheshwari PH, Dhama TL, Tandon RP (2007) Characteristics of the carbon paper heat-treated to different temperatures and its influence on the performance of PEM fuel cell. *Electrochim Acta* 52:4809–4817
- Kim H, Lee YJ, Lee DC, Park GG, Yoo Y (2013) Fabrication of the carbon paper by wet-laying of ozone-treated carbon fibers with hydrophilic functional groups. *Carbon* 60:429–436
- Park SJ, Chang YH, Chang YH Moon CW, Suh DH, Im SS, Kim YC (2010) A study of atmospheric plasma treatment on surface energetics of carbon fibers. *Bull Korean Chem Soc* 31:335–338
- Osbeck S, Bradley RH, Liu C, Idriss H, Ward S (2011) Effect of an ultraviolet/ozone treatment on the surface texture and functional groups on polyacrylonitrile carbon fibres. *Carbon* 49:4322–4330
- Mathur RB, Bahl OP, Sivaram P (1992) Thermal degradation of polyacrylonitrile fibres. *Curr Sci* 62:662–669
- Yue ZR, Jiang W, Wang L, Gardner SD, Pittman CU Jr (1999) Surface characterization of electrochemically oxidized carbon fibers. *Carbon* 37:1785–1796
- Morita K, Murata Y, Ishitani A, Murayama K, Ono T, Nakajima A (1986) Characterization of commercially available PAN(polyacrylonitrile)-based carbon fibers. *Pure Appl Chem* 58:455–468
- Jones C (1991) The chemistry of carbon fibre surfaces and its effect on interfacial phenomena in fibre/epoxy composites. *Compos Sci Technol* 42:275–298

21. Gardner SD, Singamsetty CSK, Booth GL, He GR, Pittman CU Jr (1995) Surface characterization of carbon fibers using angle-resolved XPS and ISS. *Carbon* 33:587–595
22. Jones C, Sammann E (1990) The effect of low power plasmas on carbon fibre surfaces. *Carbon* 28:509–514
23. Gostick JT, Fowler MW, Ioannidis MA, Pritzker MD, Volkovich YM, Sakars A (2006) Capillary pressure and hydrophilic porosity in gas diffusion layers for polymer electrolyte fuel cells. *J Power Sources* 156:375–387
24. Fishman Z, Hinebaugh J, Bazylak A (2010) Microscale tomography investigation of heterogenous porosity distribution of PEMFC GDLs. *J Electrochem Soc* 157:B1643–B1650
25. Gostick JT, Fowler MW, Pritzker MD, Ioannidis MA, Behra LM (2006) In-plane and through-plane gas permeability of carbon fiber electrode backing layers. *J Power Sources* 162:228–238
26. Yim SD, Kim BJ, Sohn YJ, Yoon YG, Park GG, Lee WY, Kim CS, Kim YC (2010) The influence of stack clamping pressure on the performance of PEM fuel cell stack. *Curr Appl Phys* 10:S59–S61
27. Hwang GS, Weber AZ (2012) Effective-diffusivity measurement of partially-saturated fuel-cell gas-diffusion layers fuel cells, electrolyzers, and energy conversion. *J Electrochem Soc* 159:F683–F692